DOI: 10.2352/ISSN.2470-1173.2016.12.IMSE-269

Miniature lensless computational infrared imager

Evan L. Erickson, Mark D. Kellam, Patrick R. Gill, James Tringali,* and David G. Stork**
*Rambus Labs, 1512 East Franklin Street #200, Chapel Hill, NC 27514 and *1050 Enterprise Way, Suite 700, Sunnyvale, CA 94089*

Abstract

*We describe a lensless computational far-field imager that responds to thermal infrared light (*8–14 μm*) and comprises a spiral binary phase grating integrated with an* 80×80*-pixel microbolometer array followed by Fourier-domain computational image reconstruction. We believe this is the first hardware demonstration of computational diffractive imaging in thermal infrared.*

Background: Computational imaging

Computational imaging is the technological discipline in which both optical hardware and digital signal processing are jointly designed for a desired end-to-end function.[1, 21] Because the digital signal processing can assume some of the burden of image feature extraction or overall image creation that is traditionally assumed by optical devices such as lenses or curved mirrors, the design constraints on optical hardware can be relaxed, thereby expanding opportunities in size and form factor, or reducing hardware complexity and cost. In this approach there is no need for the intermediate optical image to "look good," but instead merely to carry the information needed to *compute* the digital image. True joint design seeks the optimal tradeoff between hardware and signal processing, where each performs the portion of the complete image creation for which it is best suited. For instance, chromatic aberration is difficult to correct by lenses but rather simple to correct by digital processing while coma aberration is the reverse.[14] Computational imaging can provide novel image functionality, and exploit novel optical elements such as cubic phase plates for extended depth of field,[2] coded apertures for compressive sensing and motion capture,[11] structured lighting for depth estimation,[3] and more.

Computational imaging has been applied to the design of *lensless diffractive* imagers as well. In lensless microscopy, a small sample, such as a biological cell, is placed close to a photodetector array; coherent or partially coherent illumination scatters off the sample and interferes with the unscattered illumination to form a holographic interference pattern on the photodetector array. Computational deconvolution of the sensed pattern yields an estimate of the amplitude or phase profile of the sample.[15]

Far-field lensless diffractive imaging—our central concern here—has been demonstrated in the visible spectrum.[6, 9, 7, 8, 17, 18] This approach has better wavelength independence than comparable micro-lens or Fresnel zone plate methods.[16] Moreover, such diffractive computational sensing can be generalized to new types of gratings and processing matched to a specific sensing task, such as QR code reading and visual line position estimation.[19, 13]

The thermal infrared sensor reported here has the same fundamental architecture and processing as earlier systems that sense the visible spectrum,[18, 5, 10, 20] but differs in a number of properties, such as the sensor array technology, as we shall see.

Computational diffractive imaging: Theory

We model the image acquisition pathway as a linear system, $\mathbf{y} = \mathbf{A}\mathbf{x} + \mathbf{n}$, where the $\mathbf{y}$ represents the (microbolometer) sensor readings, $\mathbf{x}$ the thermal distribution in the input scene, and $\mathbf{n}$ sensor noise—all $n \times n$-dimensional vectors, where n is the number of pixels on one edge of our square microbolometer, while the $n^2 \times n^2$-dimensional system matrix $\mathbf{A}$ is determined by the point-spread functions due to the grating and other optical properties.

Image computation is the process of finding an estimate of the scene, $\hat{\mathbf{x}}$, given a measured sensor signal $\mathbf{y}$. Different such methods trade reconstruction accuracy (measured, for example, by a mean-squared error) versus computational cost, and are more or less appropriate according to the scene statistics as well as the symmetry, expected noise, and other properties of the overall sensor system. The most general linear image computation method is based on Tikhonov regularization, which makes least assumptions about the system.[7]

The infrared system described here is approximately shift-invariant—that is, the point spread function does not vary significantly throughout the microbolometer area—and thus image computation can be performed in the Fourier domain.[9, 1] Let $\mathbf{PSF}(x,y)$ denote the (shift-invariant) point spread function (Fig. 4) and $\mathbf{P}(\omega_x,\omega_y) = \mathscr{F}[\mathbf{PSF}(x,y)]$ its two-dimensional Fourier transform. The Fourier transform of the sensor output is $\mathbf{Y}(\omega_x,\omega_y) = \mathscr{F}[\mathbf{y}(x,y)]$. Finally, the Fourier transform of the deconvolution kernel is then

$$\mathbf{K}(\omega_x,\omega_y) = \frac{\mathbf{P}^*(\omega_x,\omega_y)}{\gamma + |\mathbf{P}(\omega_x,\omega_y)|^2}, \tag{1}$$

where * denotes complex conjugation and γ is a scalar regularization parameter whose optimal value depends upon the statistics of the scene and the noise $\mathbf{n}$. The estimate of the scene is then efficiently computed in the Fourier domain by

$$\hat{\mathbf{x}} = \mathscr{F}^{-1}[\mathbf{Y} \cdot \mathbf{K}]. \tag{2}$$

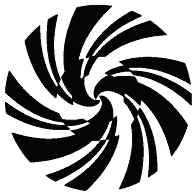

Figure 1. *The phase anti-symmetric spiral grating design in our thermal IR sensor consists of three annular regions of different spatial complexity. Here the black and white representation a phase difference of* $\lambda/2 \approx 5\ \mu m$*, corresponding to the middle of the infrared wavelength range of interest.[8]*

DOI: 10.2352/ISSN.2470-1173.2016.12.IMSE-269

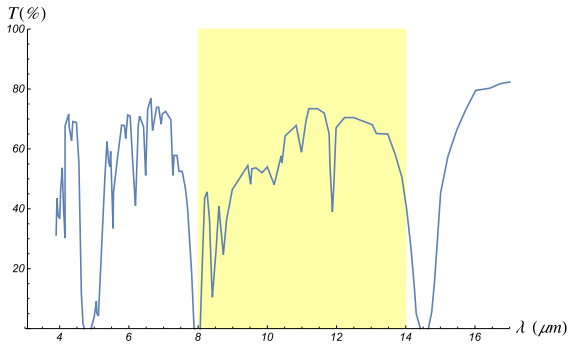

Figure 2. *Transmittance of Poly IR® 2 for a sample thickness of* $0.38\ mm$*, where the yellow highlighting corresponds to the spectral range of the sensitivity of the Sofradir microbolometer array. (Replotted from FresnelTech, Inc. data.)*

Infrared sensor hardware

Spiral anti-symmetric phase gratings capture the full spatial Fourier information up to the Nyquist rate of the microbolometer (Fig. 1).[7] Our grating is made of Poly IR® 2 material (index of refraction $n = 1.54$) which has broad transmittance in the thermal infrared (Fig. 2). The material was stamped with a binary phase-antisymmetric spiral scaled larger from our earlier visible-spectrum designs for the thermal infrared wavelengths of interest here. Such gratings have uniquely optimal properties of robustness to manufacturing variations and to wavelength variations.[4] Our images are "panchromatic," that is, in a one-dimensional scale in temperature. The grating layer is roughly $254\ \mu m$ thick and mounted to a Sofradir ATOM80 uncooled microbolometer array having a pixel pitch of $34\ \mu m$; the overall sensor is $2.72 \times 2.72\ mm^2$ with a circular grating aperture of $2.096\ mm$ diameter with an effective optical speed of $f/1.1$.

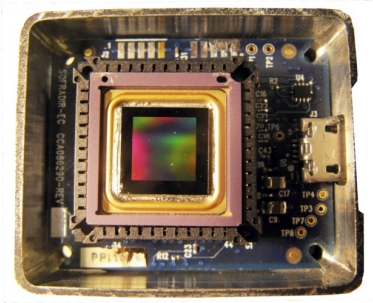

Figure 3. *The sensor assembly consists of a Sofradir ATOM80 microbolometer, which has a spectral response of* $8\text{–}14\ \mu m$ *and noise-equivalent temperature difference or NETD of roughly* $100\ mK$ *at* $f/1$ *and* $27°C$*. The phase grating is not shown.*

The Sofradir microbolometer array has 14-bit pixels and a frame rate of $9\ fps$. Our *Matlab* code can process 200×200-pixel data in $2\ ms$—well above video rates. Figure 3 shows the sensor assembly, microbolometer array, printed circuit board and support electronics.

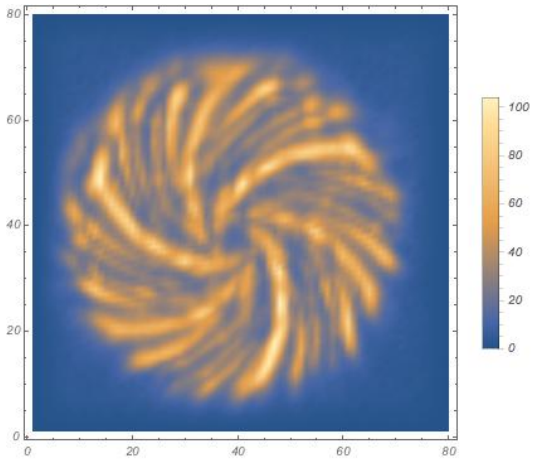

Figure 4. *The empirical point-spread function for broad-band thermal infrared illumination and the phase grating shown in Fig. 1 for a point source at the center of the field of view. We found that this point-spread function is effectively spatially invariant throughout the field of view. Note from the scale bar that all values are non-negative for a microbolometer.*

Image signal processing

Sensor calibration consists of measuring the point-spread function $\mathbf{PSF}(x,y)$, that is, the response to a plane wave or distant point source; calibration need be done just once. The basic image computation is governed by Eq. 2 but here with two slight modifications required to compensate for properties of our specific sensor. First, the fact that the point-spread function covers a large portion of the microbolometer sensor area means that for large field angles (large angles of incidence) much of the refracted and diffracted infrared radiation falls outside the sensor area. (The effect of the loss of signal information is less than in the case of an arbitrary point-spread function.) By design, the point-spread function in Fig. 4 is radially symmetric, and thus even as much as one half of the point-spread function falls outside the microbolometer array the other half is capturing the same two-dimensional spatial frequencies, though with lower signal-to-noise. Nevertheless, a simple application of Eq. 2 would lead to visual artifacts from Gibbs ringing. We reduced such artifacts by mirroring the data corresponding to the area outside the microbolometer, and by artificially vignetting the signal near the periphery by a spatially separable function.

The field of view of our sensor is rather narrow: $\pm 14°$, but this is not a fundamental limitation of the design. The field of view depends upon the geometry of the grating, in particular the distance between the microbolometer pixels and the top of the infrared window. Simulations show that such sensors could be made to have fields of view as large as $\pm 60°$.

Imaging results

Figure 6 shows raw sensor readings (without computational vignetting) for a complex scene consisting of a human hand in front of a uniform background. (The scale is in arbitrary units.) All fingers and the thumb are visible and the shape defined enough that simple intensity based edge detection and thresholding can segment the hand from the background.

DOI: 10.2352/ISSN.2470-1173.2016.12.IMSE-269

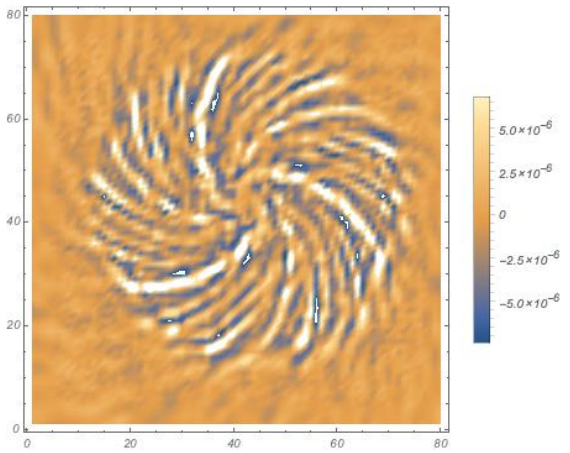

Figure 5. *The deconvolution kernel—the inverse Fourier transform of* $\mathbf{K}(\omega_x, \omega_y)$ *in Eq. 1—for the empirical point-spread function in Fig. 4. Note from the scale bar that the kernel values are both positive and negative. Roughly speaking, this kernel is a locally high-pass version of the empirical point-spread function.*

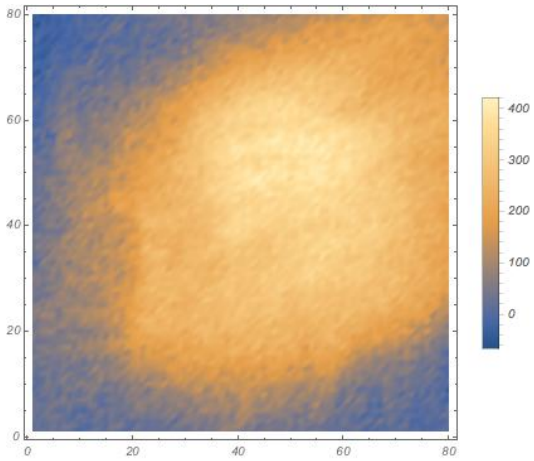

Figure 6. *The raw sensor signal* $\mathbf{y}$ *from the* 80×80*-element microbolometer array (after calibration by subtraction of a cold image and pixel linearization) including sensor and other noise.*

Figure 7 shows an 80×80-pixel reconstruction of a hand in the center of a uniform field using the image reconstruction algorithm described above. All computations were performed at 9 *f ps* on an Intel Xeon E5 processor personal computer. Although this image is somewhat noisy and of low resolution, the image is likely adequate for sensing and simple computer vision tasks such as image change detection, motion estimation and object tracking.

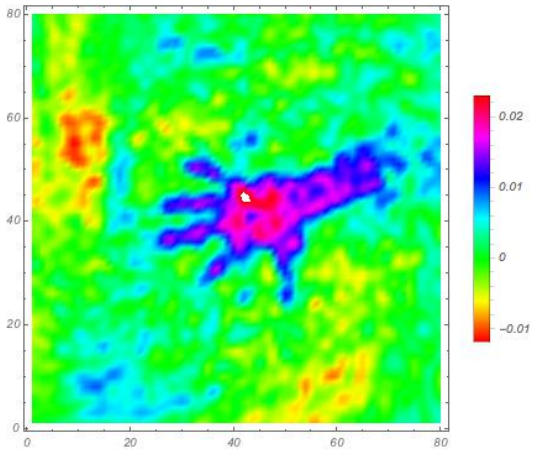

Figure 7. *The final reconstructed image, showing a hand in profile in front of a uniform scene. The field of view is* $\pm 14°$.

Conclusions and future directions

To our knowledge, the system described above represents the first demonstration of lensless computational diffractive thermal infrared imaging. Due to the nature of computational image reconstruction in noisy environments, this architecture will be most suited to wide-angle low-resolution imaging and sensing. The angle of view can be controlled by adjusting the separation between the grating and the microbolometer. The image quality can be improved with refinements of the grating design, lower-noise sensors, and improved image reconstruction methods, including ones that incorporate priors from the scene. With minor adjustments, the central architecture can exploit a range of detection technologies including thermopiles and microbolometers according to application budget, wavelength sensitivity spectrum, signal-to-noise and other requirements.[12]

A large number of applications of such technology come to mind in the broad domains of surveillance, automotive imaging (interior and exterior), machine inspection, food monitoring, internet of things, and elsewhere, such as face presence detection, people counting, and infrared image change detection. In many of these applications a low-resolution thermal image suffices when cost and form factor preclude the use of lensed systems.

Acknowledgments

We thank Thomas Vogelsang and Gary Bronner of Rambus Labs for organizational support and Fresnel Technologies, Inc., 10x MicroStructures and MCSP for prototyping assistance.

References

[1] D. J. Brady. *Optical imaging and spectroscopy*. Wiley and Optical Society of America, New York, NY, 2009.

[2] W. T. Cathey and E. R. Dowski, Jr. A new paradigm for imaging systems. *Applied Optics*, 42(29):6080–6092, 2002.

[3] J. Geng. Structured-light 3D surface imaging: A tutorial. *Advances in Optics and Photonics*, 3(2):128–160, 2011.

[4] P. R. Gill. Odd-symmetry phase gratings produce optical nulls uniquely insensitive to wavelength and depth. *Optics Letters*, 38(12):2074–2076, 2013.

[5] P. R. Gill, M. Kellam, J. Tringali, T. Vogelsang, E. Erickson, and D. G. Stork. Computational diffractive imager with low-power image change detection. In *Computational Optical Sensing and Imaging (COSI)*, Alexandria, VA, 2015.

[6] P. R. Gill and D. G. Stork. Digital camera with odd-symmetry spiral phase gratings supports full-resolution computational refocusing. In *Advanced Photonics (Optical Society of America Sensors Congress)*, 2013.

DOI: 10.2352/ISSN.2470-1173.2016.12.IMSE-269

[7] P. R. Gill and D. G. Stork. Lensless ultra miniature imagers using odd-symmetry phase gratings. In *Proceedings of Computational Optical Sensing and Imaging (COSI)*, Alexandria, VA, 2013.

[8] P. R. Gill and D. G. Stork. Hardware verification of an ultra-miniature computational diffractive imager. In *Proceedings of Computational Optical Sensing and Imaging (COSI)*, Kohala Coast, HI, 2014.

[9] P. R. Gill and D. G. Stork. Computationally efficient Fourier-based image reconstruction in a lensless diffractive imager. In *Computational Optical Sensing and Imaging (COSI)*, Arlington, VA, 2015.

[10] P. R. Gill and D. G. Stork. Depth from disparity using ultra-miniature computational diffractive sensors. In *Frontiers in Optics*, San Jose, CA (submitted), 2015.

[11] S. R. Gottesman and E. E. Fenimore. New family of binary arrays for coded aperture imaging. *Applied Optics*, 28(20):4344–4352, 1989.

[12] A. Graf, M. Arndt, M. Sauer, and G. Gerlach. Review of micromachined thermopiles for infrared detection. *Measurement Science and Technology*, 18(7):R59, 2007.

[13] M. Monjur, L. Spinoulas, P. R. Gill, and D. G. Stork. Ultra-miniature, computationally efficient diffractive visual-bar-position sensor. In *SensorComm 2015*, Venice, Italy, 2015.

[14] M. D. Robinson and D. G. Stork. Joint design of lens systems and digital image processing. In G. G. Gregory, J. M. Howard, and R. J. Koshel, editors, *SPIE International Optical Design Conference*, volume 6342, pages 6342 1G1–6342 1G10, Vancouver, BC, 2006.

[15] S. Seo, T.-W. Su, D. K. Tseng, A. Erlingera, and A. Ozcan. Lensfree holographic imaging for on-chip cytometry and diagnostics. *Lab on a Chip*, 9(6):777–787, 20109.

[16] L. Spinoulas, O. Cossairt, P. R. Gill, D. G. Stork, and A. K. Katsaggelos. Performance comparison of ultra-miniature diffraction gratings with lenses and zone plates. In *Proceedings of Computational Optical Sensing and Imaging (COSI)*, Alexandria, VA, 2015.

[17] D. G. Stork. Joint optics/signal processing design for computational diffractive sensing and imaging. In *Computational Optical Sensing and Imaging (COSI)*, Kohala Coast, HI, 2014.

[18] D. G. Stork and P. R. Gill. Optical, mathematical and computational foundations of lensless ultra-miniature diffractive imagers and sensors. *International Journal on Advances in Systems and Measurements*, 7(3-4):201–208, 2014.

[19] D. G. Stork and P. R. Gill. Reading QR code symbols with an ultra-miniature computational diffractive imager. In *Proceedings of Computational Optical Sensing and Imaging (COSI)*, Kohala Coast, HI, 2014.

[20] D. G. Stork and P. R. Gill. Computational diffractive sensing and imaging: Using optics for computation and computation for optics. In *Society for Information Display (SID)*, San Jose, CA, 2015.

[21] D. G. Stork and M. D. Robinson. Theoretical foundations of joint design of electro-optical imaging systems. *Applied Optics*, 47(10):B64–75, 2008.

Author Biography

Evan L. Erickson *is Systems Engineer at Rambus. He earned his bachelor's and master's degrees in Computer Engineering and his Ph.D. in Electrical Engineering from North Carolina State University in Raleigh. Erickson is a member of the IEEE and his research interests include computational imaging, low-power system design and high-speed signaling.*

Mark D. Kellam *is a Technical Director in Rambus Labs. He earned his Ph.D. in solid state physics as a UNC Board of Governors Fellow from the University of North Carolina at Chapel Hill. He has contributed broadly in the areas of semiconductor device design and fabrication at the Microelectronics Center of North Carolina, Charles and Colvard, and Velio Communications. His research interests include multi-physics simulations, novel emerging memory devices, and non-imaging optics.*

Patrick R. Gill *is a Principal Research Scientist at Rambus. He earned his honors bachelor's degree in physics and mathematics from the University of Toronto and his Ph.D. in biophysics studying systems neuroscience at the University of California at Berkeley and then performed postdoctoral work on tiny diffractive optics at Cornell University. Gill has won Canadian national championships in physics and mathematics, and is a member of the Optical Society of America (OSA) and IEEE.*

James Tringali *is a graduate in Electrical Engineering from the University of California, Irvine. A charter member of Rambus Labs, James is currently a Senior Manager of Systems Research. He has been a key contributor at companies such as Apple, Silicon Graphics and SanDisk and is also a veteran of three successful startup ventures: FileNet, MIPS and Matrix Semiconductor. Tringali is a member of the IEEE and ACM.*

David G. Stork *is Rambus Fellow in Rambus Labs. He is a graduate in physics from MIT and the University of Maryland and a Fellow of SPIE, the International Academy, Research and Industry Association (IARIA), the International Association of Pattern Recognition (IAPR), and Optical Society of America (OSA) as well as Senior Member of IEEE and Member of the Association for Computing Machinery (ACM) and International Society for Imaging Science and Technology (IS&T). Stork's research interests include computational imaging, machine learning, pattern classification, image analysis and computer vision, including their application to the study of fine art.*